Table 4
Mutation spectra of male *gpt* delta rats treated with NFT, NFA, or AHD for 4 weeks.

	Control		NFT		NFA		AHD	
	Number (%)	Specific mutation frequency ($\times 10^{-5}$)	Number (%)	Specific mutation frequency ($\times 10^{-5}$)	Number (%)	Specific mutation frequency ($\times 10^{-5}$)	Number (%)	Specific mutation frequency ($\times 10^{-5}$)
Base substitution								
Transversions								
G:C-T:A	3(23.1)	0.04 ± 0.04[a]	8(25.0)	0.13 ± 0.06	2(15.4)	0.03 ± 0.04	5(27.8)	0.07 ± 0.07
G:C-C:G	0	0	10(31.3)	0.16 ± 0.14**	0	0	0	0
A:T-T:A	1(7.7)	0.02 ± 0.04	3(9.4)	0.03 ± 0.08	0	0	0	0
A:T-C:G	0	0	0	0	1(7.7)	0.02 ± 0.05	1(5.6)	0.01 ± 0.02
Transitions								
G:C-A:T	6(46.2)	0.08 ± 0.05	3(9.4)	0.05 ± 0.03	7(53.8)	0.14 ± 0.11	8(44.4)	0.09 ± 0.08
A:T-G:C	1(7.7)	0.01 ± 0.03	3(9.4)	0.05 ± 0.03	1(7.7)	0.02 ± 0.05	2(11.1)	0.04 ± 0.06
Deletion								
Single bp	2(15.4)	0.01 ± 0.03	3(9.4)	0.04 ± 0.05	0	0	1(5.6)	0.01 ± 0.02
Over 2 bp	0	0	0	0	0	0	0	0
Insertion	0	0	1(3.1)	0.01 ± 0.02	0	0	0	0
Complex	0	0	1(3.1)	0.02 ± 0.04	2(15.4)	0.03 ± 0.06	1(5.6)	0.02 ± 0.04
Total	9	0.17	32	0.49	13	0.25	18	0.24

[a] Means ± SD.
** Significantly different ($P < 0.01$) from the control group by Steel's test.

2.5. Measurement of 8-OHdG

Kidney DNA of male or female *gpt* delta rats was extracted and digested as described previously (Umemura et al., 2003). In brief, renal DNA was extracted with a DNA extractor WB kit (Wako Pure Chemical Inc., Osaka, Japan) containing an oxidant NaI solution to dissolve cellular components. For prevention of auto-oxidation, deferoxamine mesylate (Sigma Chemical, MO, USA) was added to the lysis buffer. The collected DNA pellet was digested into deoxynucleosides by treatment with nuclease P1 and alkaline phosphatase. Digested DNA was measured for 8-OHdG (8-OHdG/10^5 dG) levels by high-performance liquid chromatography with an electrochemical detection system (Coulochem II; ESA, Bedford, MA, USA) as previously reported (Umemura et al., 2006).

2.6. Histopathology

Fixed kidney tissues were embedded in paraffin, and after sectioning into 4 μm thick sections, samples were stained with hematoxylin and eosin (H&E) according to a conventional method and were examined histopathologically.

Table 5
Mutation spectra of male *gpt* delta rats treated with NFT, NFA, or AHD for 13 weeks.

	Control		NFT		NFA		AHD	
	Number (%)	Specific mutation frequency ($\times 10^{-5}$)	Number (%)	Specific mutation frequency ($\times 10^{-5}$)	Number (%)	Specific mutation frequency ($\times 10^{-5}$)	Number (%)	Specific mutation frequency ($\times 10^{-5}$)
Base substitution								
Transversions								
G:C-T:A	3(20.0)	0.05 ± 0.07[a]	7(31.8)	0.65 ± 0.60*	3(20.0)	0.18 ± 0.16	1(11.1)	0.02 ± 0.05
G:C-C:G	0	0	7(31.8)	0.51 ± 0.17*	0	0	0	0
A:T-T:A	2(13.3)	0.02 ± 0.04	1(4.5)	0.06 ± 0.12	2(13.3)	0.10 ± 0.22	0	0
A:T-C:G	1(6.7)	0.01 ± 0.02	0	0	1(6.7)	0.05 ± 0.11	0	0
Transitions								
G:C-A:T	5(33.3)	0.18 ± 0.31	4(18.2)	0.32 ± 0.32	4(26.7)	0.21 ± 0.21	5(55.6)	0.26 ± 0.32
A:T-G:C	2(13.3)	0.02 ± 0.03	0	0	2(13.3)	0.10 ± 0.22	0	0
Deletion								
Single bp	1(6.7)	0.04 ± 0.10	2(9.1)	0.22 ± 0.37	1(6.7)	0.05 ± 0.11	3(33.3)	0.15 ± 0.21
Over 2 bp	0	0	1(4.5)	0.06 ± 0.12	0	0	0	0
Insertion	0	0	0	0	0	0	0	0
Complex	1(6.7)	0.04 ± 0.08	0	0	2(13.3)	0.11 ± 0.16	0	0
Total	15	0.35	22	1.82	15	0.80	9	0.43

[a] Means ± SD.
* Significantly different ($P < 0.05$) from the control group by Steel's test.

Table 6
Spi⁻ MFs in the kidneys of male *gpt* delta rats treated with NFT, NFA, or AHD for 4 weeks.

Treatment	Animal No.	Plaques within XL-1 Blue MRA ($\times 10^5$)	Plaques within WL95 (P2)	MF ($\times 10^{-5}$)	Mean ± SD
Control	1	11.1	6	0.54	
	2	12.3	4	0.32	
	3	13.1	12	0.92	
	4	7.7	3	0.39	
	5	6.6	3	0.46	0.53 ± 0.23
NFT	11	18.1	5	0.28	
	12	10.4	4	0.39	
	14	14.4	11	0.76	
	15	6.9	3	0.43	0.46 ± 0.21
NFA	21	8.6	3	0.35	
	22	11.7	7	0.60	
	24	5.6	9	1.61	
	25	5.2	2	0.38	0.74 ± 0.60
AHD	31	11.1	6	0.54	
	32	9.7	2	0.21	
	33	13.3	2	0.15	
	34	10.4	2	0.19	
	35	7.0	11	1.57	0.53 ± 0.60

MF, mutant frequency.

2.7. Immunohistochemical staining for α_{2u}-globulin

Kidney sections of NFT-treated male *gpt* delta rats were immunostained with a polyclonal anti-rat-α_{2u}-globulin antibody. Antigen retrieval was carried out by microwaving for 10 min in pH 6.0 citrate buffer. Sections were incubated with anti-rat-α_{2u}-globulin antibody (1:200 dilution in PBS, R&D Systems, Inc., MN, USA) overnight at 4 °C and then incubated with substrate solution containing an enzyme-labeled secondary antibody for 30 min at room temperature (N-Histofine Simple Stain, Nichirei Biosciences Inc., Tokyo, Japan). Finally, sections were counter-stained with hematoxylin for microscopic examination.

2.8. Western blot analysis for α_{2u}-globulin

Kidney tissues of male and female rats were homogenized in RIPA buffer (50 mmol/l Tris–HCl pH 8.0, 150 mmol/l sodium chloride, 0.5 w/v% sodium deoxycholate, 0.1 w/v% sodium dodecyl sulfate, 1.0 w/v% NP-40; Takara Bio Inc., Shiga, Japan) containing 1% protease inhibitor cocktail (Sigma Chemical Co.). The homogenate was centrifuged for 30 min at 10,000 × *g* at 4 °C, and the supernatant was collected. Protein concentrations were measured with a Multiskan FC (Thermo Fisher Scientific Inc., MA, USA) for the BCA protein assay using advanced protein assay reagent (Cytoskelton Inc. CO, USA). Kidney proteins were diluted with

Table 7
Spi⁻ MFs in the kidneys of male *gpt* delta rats treated with NFT, NFA, or AHD for 13 weeks.

Treatment	Animal No.	Plaques within XL-1 Blue MRA ($\times 10^5$)	Plaques within WL95 (P2)	MF ($\times 10^{-5}$)	Mean ± SD
Control	6	5.0	5	1.01	
	7	10.4	3	0.29	
	8	4.4	2	0.45	
	9	56.7	2	0.35	
	10	5.1	4	0.78	0.58 ± 0.31
NFT	17	4.3	3	0.69	
	18	9.7	9	0.93	
	19	5.7	5	0.88	
	20	5.3	9	1.69	1.05 ± 0.44
NFA	26	14.9	16	1.08	
	27	11.1	12	1.08	
	28	14.8	31	2.10	
	29	3.9	3	0.78	
	30	2.8	2	0.72	1.15 ± 0.56
AHD	36	3.7	2	0.54	
	37	6.1	2	0.33	
	38	22.6	81	3.59	
	39	3.1	2	0.65	
	40	4.2	1	0.24	1.07 ± 1.42

MF, mutant frequency.

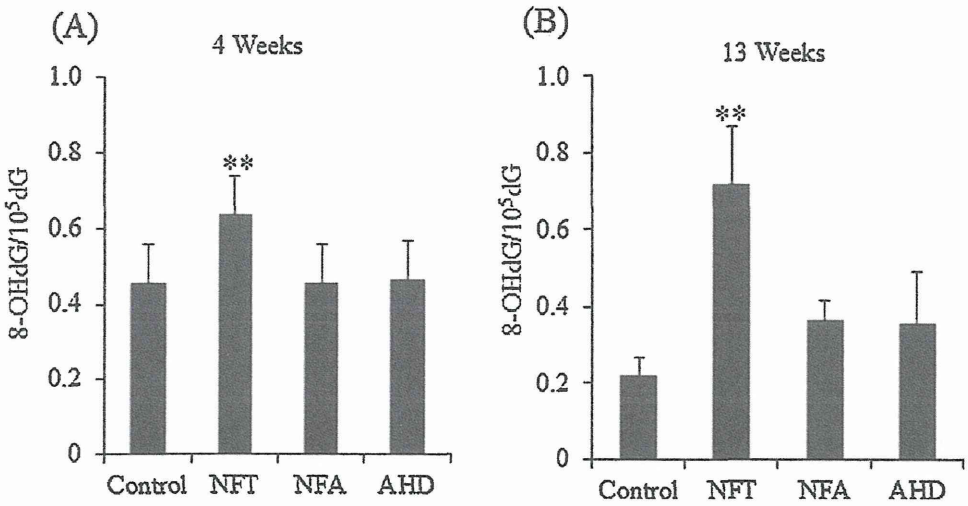

Fig. 3. 8-OHdG levels in the kidneys of male F344 *gpt* delta rats treated with NFT, NFA, or AHD for 4 (A) or 13 (B) weeks. Values are means ± SD for 5 rats, (4 rats; NFT (A, B) and NFA (A)). ** Significantly different ($P < 0.01$) from the control group by Dunnett's test.

sample buffer (BIO-RAD, CA, USA) containing 2-mercaptoethanol, heated for 2 min at 95 °C, and then quenched. Samples containing total proteins of 0.5 μg were electrophoresed on 4–15% sodium dodecyl sulfate-polyacrylamide (SDS) gradient gel (BIO-RAD) and were transferred to a polyvinylidene difluoride (PVDF) membrane (EMD Millipore, Germany) using a semi-dry blotting system. After blocking with 0.5% casein-TBS-T for 1 h at room temp, the membrane was incubated with anti-rat-α_{2u}-globulin (1:200 dilution in blocking buffer, R&D Systems, Inc. USA) overnight at 4 °C. The membrane was incubated with peroxidase-conjugated secondary antibody, polyclonal-anti-goat IgG (1:2000 dilution in blocking buffer, Dako Japan Inc.) for 1 h at room temp. Recognized protein bands were visualized with ECL-prime reagents (GE Healthcare, NJ, USA), and specific bands were detected with BIO-RAD Molecular Image ChemiDoc™ XRS+ with Image Lab™ Software.

2.9. Statistical analysis

The body and kidney weights, serum biochemistry, 8-OHdG levels, *gpt* and Spi⁻MFs, and *gpt*-mutation spectra are presented as means ± SD. All data were evaluated for consistency with a normal distribution and variance homogeneity using Levene's test or visual examination of a scatter plot. The presence or absence of outliers was confirmed visually from the same scatter plot. The data in experiment 1 were analyzed with Dunnett's multiple comparison test, and when normality or variance homogeneity was an issue, they were analyzed with Steel's test. The data in experiment 2 between controls and the NFT-treated group were analyzed with the Student's *t*-test or Wilcoxon rank sum test.

3. Results

3.1. Experiment 1

3.1.1. General conditions, food consumption, body and kidney weights

Although the cause of death was not able to be determined, deaths of NFT-treated rats occurred with one male rat at both weeks 3 and 5, and one NFA treated rat died at week 3. The change in body weights and food consumption after 13 weeks is shown in Fig. 2. In the NFT or NFA treated groups, small increased rates of body weight gain compared to the control group were observed. Food consumption was similar for all groups. The final mean body weights of male rats that received NFT, NFA, or AHD for 13 weeks were 18%, 11%, or 2.6% lower than that of controls, respectively (Table 1). Relative kidney weights were significantly increased in the NFT and NFA group at week 13 (Table 1).

3.1.2. In vivo *mutation assay of kidneys*

Results of the *gpt* assay with male rats treated with NFT, NFA, or AHD for 4 or 13 weeks are shown in Tables 2 and 3. In the NFT-treated group, the *gpt* MF was 3 times higher than in the control group at week 4. The *gpt* MF in the NFT group at week 13 was 5 times higher than in the control group and was statistically significant. Notably, an increase in *gpt* MF was observed in the NFA-treated group at week 13, but was not observed in the AHD-treated group. Tables 4 and 5 show the results of spectrum analysis of *gpt* mutants observed at week 4 or 13. NFT caused an increase in G-base substitution mutations compared with control; G:C-C:G and G:C-T:A transversion mutations were significant at weeks 4 and 13, respectively. These G-base substitution mutations accounted for

Table 8
Histopathological findings in the kidneys of male *gpt* delta rats treated with NFT, NFA, or AHD for 4 or 13 weeks.

		4 Weeks				13 Weeks			
	Group	Control	NFT	NFA	AHD	Control	NFT	NFA	AHD
	No. of animals	5	4	4	5	5	4	5	5
	Grade								
Hyaline droplet, proximal tubule	±	5	–	1	5	5	–	1	5
	+	–	3	3	–	–	–	4	–
	++	–	1	–	–	–	4	–	–

±, Very slight; +, Slight; ++, Moderate.

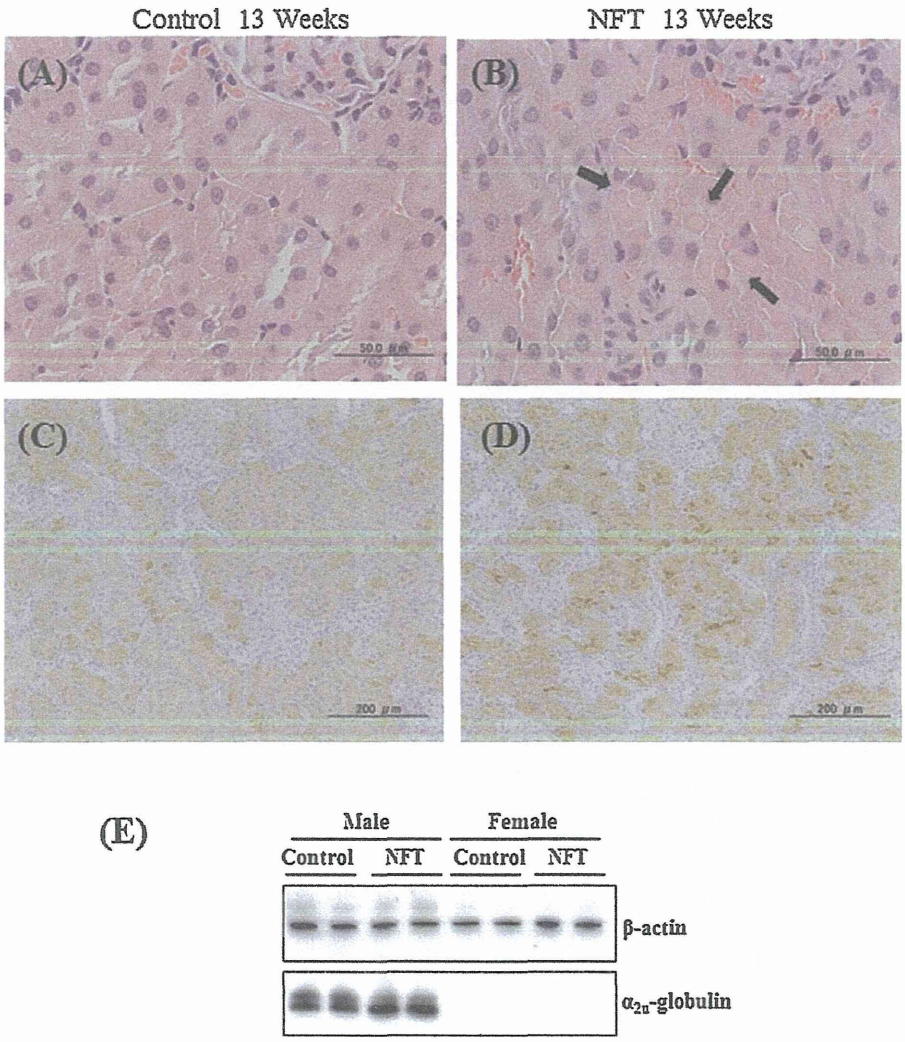

Fig. 4. Histopathological features from H&E staining (A, control; B, NFT-treated), and photomicrographs of immunohistochemical staining a_{2u}-globulin (C, control; D, NFT-treated) of the kidneys of male F344 *gpt* delta rats at week 13. Note (B) hyaline droplets in the proximal tubules (arrow head) were observed. Western blotting analysis for a_{2u}-globulin (E). Note (E) kidney protein samples of the controls and NFT-treated rats at week 13 are shown with samples from each sex. a_{2u}-globulins of 15.5 and 18.7 kDa were detected only in males, and NFT treatment caused an increase in the 15.5 kDa protein.

a higher percentage in the total *gpt* mutants observed in the NFT-treated group, and were 56% and 64% at weeks 4 and 13, respectively. In the Spi$^-$ assay, no significant changes in Spi$^-$ MF were observed in rats treated with NFT, NFA, or AHD compared with controls after administration for 4 (Table 6) and 13 weeks (Table 7).

3.1.3. Measurement of 8-OHdG in kidney DNA

8-OHdG levels in NFT-treated rats were significantly increased after 4 weeks and significantly increased by over 3 fold compared to controls at week 13 (Fig. 3). Neither NFA nor AHD treated rats exhibited a significant change in their 8-OHdG level.

3.1.4. Histopathologic examination of kidneys, including immunostaining of α_{2u}-globulin

The results of histopathological examinations of the kidneys are shown in Table 8. NFT treatment caused an increase in the number of hyaline droplets in the proximal tubules depending on the treatment period (Fig. 4A and B) and showed positive immunostaining for α_{2u}-globulin in male rat kidneys (Fig. 4C and D). Likewise, elevation of the α_{2u}-globulin protein level was confirmed by western blotting analysis, shown in Fig. 4E. α_{2u}-globulin is a major male rat specific urinary protein, which has two molecular weight types: an 18.7 kDa major urinary protein (native type) and a 15.5 kDa (kidney type) that is proteolytically modified from the native type (Wang et al., 2000; Hai and Kizilbash, 2013). The expression of this protein is well known to change in response to drug treatment. Western blotting analysis showed that NFT induced formation of the 15.5 kDa protein.

3.2. Experiment 2

3.2.1. General conditions, food consumption, body and kidney weights

No animal deaths were detected during 13 weeks of NFT administration. In the NFT-treated group, low body weight compared with the control group was noticeable from week 1 (Fig. 5), and an increase in kidney weight compared with controls was also observed (Table 9).

3.2.2. In vivo mutation assay in kidneys

Results of the *gpt* assay for the kidneys of female rats treated with NFT for 13 weeks are shown in the Table 10. With the same tendency as with males, *gpt* MFs in the NFT-treated group were significantly higher, over 5 fold compared with the control group. Increases in G-base substitution mutations, G:C-T:A and G:C-C:G

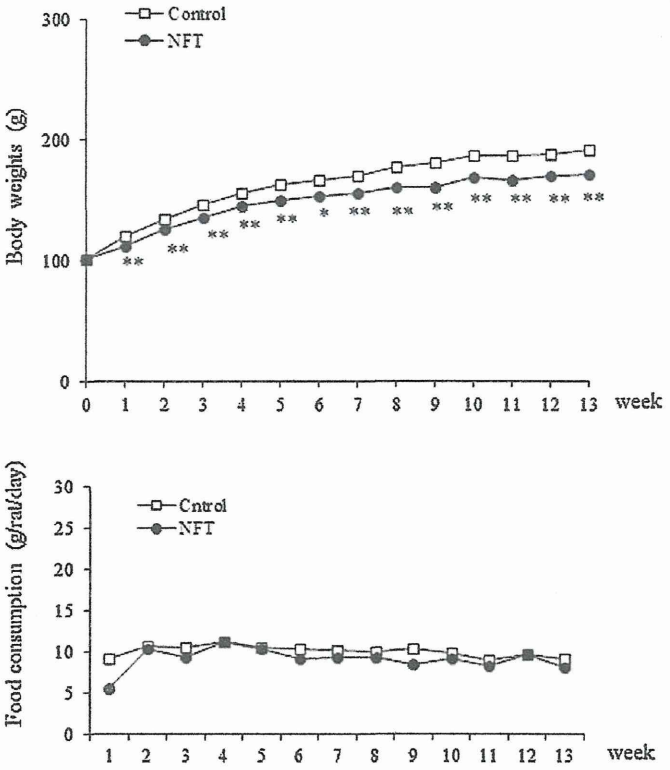

Fig. 5. Growth curves and food consumption for female *gpt* delta rats treated with NFT for 13 weeks. *,** Significantly different ($P < 0.05$, 0.01) from the control group by Student's *t*-test or the Wilcoxon rank sum test.

Table 9
Final body and kidney weights of female *gpt* delta rats treated with NFT for 13 weeks.

	Final body weight (g)	Kidney weight	
		Absolute (g)	Relative (g%)[a]
Control	191.0 ± 11.1[b]	1.10 ± 0.07	0.58 ± 0.03
NFT	171.4 ± 6.3**	1.23 ± 0.08**	0.72 ± 0.05**

[a] Kidney weight-to-body weight ratios (relative weights) are given as g organ weight/g body weight.
[b] Means ± SD.
** Significantly different ($P < 0.01$) from the control group by Student's *t*-test.

transversion mutations, were observed in female rat kidneys similar to the results with males, as shown in Table 11. Results of the Spi⁻ assay are shown in Table 12, with no significant changes in Spi⁻ MF observed in NFT-treated rats.

3.2.3. Measurement of 8-OHdG in kidney DNA

Fig. 6 shows that 8-OHdG levels in the kidneys of female rats treated with NFT for 13 weeks significantly increased to over 5 fold the level of the control group.

4. Discussion

Administration of NFT to male *gpt* delta rats at a dose corresponding to the renal carcinogenic dose in male F344 rats caused a significant increase in *gpt* MFs, but not Spi⁻ MFs, in their kidneys in a dose period-dependent manner. The significant increment of MF in the reporter gene at the carcinogenic target site strongly suggests involvement of genotoxic mechanisms in NFT-induced renal carcinogenesis. In a spectrum analysis of *gpt* mutants in NFT-treated rats, G:C-T:A and G:C-C:G transversion were the predominant mutations found. The guanine base in genomic DNA is highly responsive to various ROS and is susceptible to oxidative modification (Cheng et al., 1992; Kino and Sugiyama, 2000). In fact, 8-OHdG levels in the kidneys of NFT-treated rats were significantly increased after 4 weeks and were further elevated at 13 weeks. The present data clearly demonstrates that NFT at the carcinogenic dose is capable of generating oxidative stress leading to oxidative DNA damage at the carcinogenic target site. Considering that 8-OHdG causes G:C-T:A transversion mutations resulting from its potential for mispairing with adenine (Cheng et al., 1992), oxidative DNA damage including 8-OHdG formation might contribute to guanine base substitution mutations observed in the *gpt* gene following NFT exposure. Since contribution of 8-OHdG to carcinogenicity has been demonstrated (Umemura et al., 2006), genotoxic mechanisms including oxidative DNA damage may be involved in NFT-induced renal carcinogenesis.

Most nitro compounds, such as nitroquinone and nitro-heterocycles like nitroimidazole and nitrofurans, are considered to exert their toxic effect by nitro reduction (Bartel et al., 2009; Boelsterli et al., 2006; Chung et al., 2011). One-electron reduction of the nitro group catalyzed by nitro-reductase gives rise to nitro anion radical, the chemical instability of which promotes production of various ROS such as superoxide anion and hydroxyl radical via its electron-donating ability (Wang et al., 2008). It has been reported that the modes of action underlying DNA damage or cytotoxicity induced by NFT in rodent liver and lungs may involve ROS generation by nitro reduction (Rossi et al., 1988; Suntres and Shek, 1992). Accordingly, it is highly probable that nitro reduction

Table 10
gpt MFs in the kidneys of female *gpt* delta rats treated with NFT for 13 weeks.

Treatment	Animal No.	Cm^R colonies ($\times 10^5$)	6-TG^R and Cm^R colonies	MF ($\times 10^{-5}$)	Mean ± SD
Control	1	3.11	6	1.93	
	2	8.10	5	0.62	
	3	5.36	6	1.12	
	4	2.97	3	1.01	
	5	5.99	4	0.67	1.07 ± 0.53
NFT	6	2.88	22	7.64	
	7	N.D.	–	–	
	8	1.89	13	6.88	
	9	5.04	27	5.36	
	10	2.97	17	5.72	6.40 ± 1.05**

Cm^R, chloramphenicol resistant; 6-TG^R 6-thioguanine resistant; MF, mutant frequency; and N.D., not detected.
** Significantly different ($P < 0.01$) from the control group by Student's *t*-test.

Table 11
Mutation spectra of female *gpt* delta rats treated with NFT for 13 weeks.

	Control		NFT	
	Number (%)	Specific mutation frequency ($\times 10^{-5}$)	Number (%)	Specific mutation frequency ($\times 10^{-5}$)
Base substitution				
Transversions				
G:C-T:A	3(13.0)	0.10 ± 0.15	12(22.6)	1.01 ± 0.96*
G:C-C:G	1(4.3)	0	14(26.4)	1.18 ± 0.48*
A:T-T:A	1(4.3)	0.04 ± 0.08	2(3.8)	0.26 ± 0.53
A:T-C:G	3(13.0)	0	2(3.8)	0.26 ± 0.53
Transitions				
G:C-A:T	8(34.8)	0.31 ± 0.08	10(18.9)	0.87 ± 0.51
A:T-G:C	2(8.7)	0.10 ± 0.15	4(7.5)	0.34 ± 0.30
Deletion				
Single bp	4(17.4)	0.18 ± 0.28	5(9.4)	0.34 ± 0.46
Over 2 bp	0	0	0	0
Insertion	0	0	1(1.9)	0.07 ± 0.10
Complex	1(4.3)	0	3(5.7)	0.29 ± 0.32
Total	23	1.01	53	4.81

* Significantly different ($P < 0.05$) from the control group by Student's *t*-test.

of NFT is responsible for oxidative stress inducing oxidative DNA damage and subsequent gene mutations.

On the other hand, NFA, a constituent compound of NFT with the nitro group, was also able to induce a significant elevation of *gpt* MFs in the kidneys. However, NFA failed to increase 8-OHdG levels in the kidney DNA of *gpt* delta rats despite possessing the same nitro group as NFT. In addition, the mutation spectrum of *gpt* mutants obtained from kidney DNA in NFA-treated rats was not identical to that of NFT-treated rats. NFA has been used as a raw material for the synthesis of many nitrofurans (Cerecetto et al., 1998; Zorzi et al., 2014). Although NFA is known as a photolysis breakdown product from NFT (Busker et al., 1988; Busker and Beijersbergen van Henegouwen, 1987), it is unclear whether NFA could be a metabolite of NFT detected by *in vivo* study.

In general, the rate of nitro reduction is thought to be partly dependent on chemical structure. The inconsistent results between NFT and NFA regarding 8-OHdG formation might indicate that ROS form more readily from the nitro group of NFT. Nitro compounds are reduced to amines as the inactive form via the reactive intermediates including nitroso and hydroxylamine derivatives at multiple stages (Boelsterli et al., 2006). The fact that these reactive intermediates can directly cause nucleophilic reactions with DNA (Cerecetto and González, 2011 Hall et al., 2011; Ona et al., 2009; Streeter and Hoener, 1988) might provide a clue to explaining how NFA induces genotoxicity without oxidative DNA damage. In light of the present data that the other derivative of NFT, AHD, induced neither elevation of 8-OHdG levels nor *gpt* MFs in kidney DNA of rats, it is highly probable that NFA contains a key structural element responsible for NFT-induced genotoxicity. Namely, the mechanisms underlying NFT-induced genotoxicity may involve not only oxidative stress arising from reduction of nitro group, but also some other modes of action involved in the genotoxicity of NFA.

In the NFT-treated group, the accumulation of hyaline droplets in the proximal tubules of the kidney was a prominent feature. Immunohistochemical staining showed these droplets to be positive for α_{2u}-globulin. Western blot analysis also supported NFT being able to accumulate α_{2u}-globulin protein in the proximal tubules. It is well known that the accumulation of α_{2u}-globulin causes the proximal tubular cell injury and subsequently compensatory cell proliferation (Borghoff et al., 2001). Under conditions of the sustained high cell proliferation, it is thought that the rate of spontaneous DNA replication errors is increased (Cunningham, 1996). As a matter of fact, this is the rationale for carcinogenicity of non-genotoxic carcinogens with α_{2u}-globulin inducible potency. In addition, it has been accepted that genomic DNA in cells recruiting into the cell cycle is susceptible to DNA damage. Accordingly, the positive outcome in the reporter gene mutation assay using male rats does not always imply direct genotoxicity of NFT. Therefore, a further study using female *gpt* delta rats, in which the effects of α_{2u}-globulin were not involved, was performed to assess *in vivo* genotoxicity of NFT together with induction of oxidative DNA damage. As a result, administration of NFT to female *gpt* delta rats at the same dose used for males caused significant elevations of both 8-OHdG levels and *gpt* MFs to the same extent as for males. These data clearly showed that α_{2u}-globulin-mediated nephropathy due to NFT treatment did not affect susceptibility to NFT-induced genotoxicity. According to the carcinogenicity studies of NFT conducted by the NTP (1989), NFT was not carcinogenic to the kidneys of female rats in contrast to male rats. Accordingly, α_{2u}-globulin-mediated nephropathy may be a prerequisite for compelling initiated cells to develop neoplastic cells in NFT-induced renal carcinogenesis, *i.e.*, NFT could be a latent carcinogen in female rats, which implies that the cancer hazard to humans still exists.

Table 12
Spi MFs in the kidneys of female *gpt* delta rats treated with NFT for 13 weeks.

Treatment	Animal No.	Plaques within XL-1 Blue MRA($\times 10^5$)	Plaques within WL95 (P2)	MF ($\times 10^{-5}$)	Mean ± SD
Control	1	7.47	4	0.54	
	2	9.09	3	0.33	
	3	7.56	6	0.79	
	4	6.75	1	0.15	
	5	8.46	4	0.47	0.46 ± 0.24
NFT	6	4.14	5	1.21	
	7	3.69	2	0.54	
	8	6.30	3	0.48	
	9	6.30	2	0.32	
	10	5.04	2	0.40	0.59 ± 0.36

MF, mutant frequency.

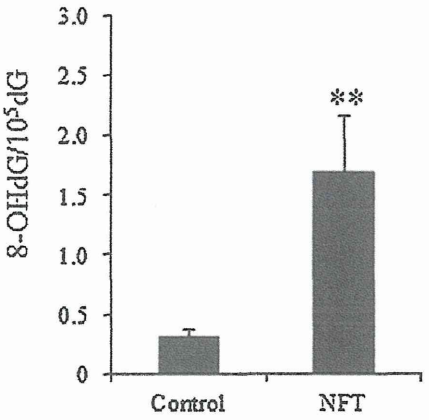

Fig. 6. 8-OHdG levels in the kidneys of female F344 *gpt* delta rats treated with NFT for 4 weeks. Values are means ± SD for 5 rats. ** Significantly different ($P < 0.01$) from the control group by Student's *t*-test.

5. Conclusion

The present study clearly demonstrated that genotoxic mechanisms were involved in NFT-induced renal carcinogenesis in rats. Among the two chemical structure-related compounds of NFT, the common structure between NFT and NFA may play a key role in NFT-induced genotoxicity and not the AHD substructure. The modes of action underlying NFT-induced genotoxicity involve not only NFA-induced genotoxic mechanisms but also oxidative DNA damage. NFT-induced carcinogenicity in rat kidney requires male rat-specific α_{2u}-globulin-mediated nephropathy, but NFT-induced genotoxicity probably occur any species. Therefore, the carcinogenic risk of NFT to humans should be of concern.

Conflict of interest

The authors declare that there are no conflicts of interest.

Transparency document

The Transparency document associated with this article can be found in the online version.

Acknowledgements

We are grateful to members of the department of pathology in NIHS for helpful support. We thank Ms. Ayako Saikawa and Ms. Yoshimi Komatsu for expert technical assistance in processing histological materials. This research was supported by a Grant-in-Aid from the Ministry of Health, Labour and Welfare, Japan (H-22-shokuhin-ippan-007, H25-shokuhin-ippan-005).

References

Bartel, L.C., Montalto de Mecca, M., Castro, J.A., 2009. Nitroreductive metabolic activation of some carcinogenic nitro heterocyclic food contaminants in rat mammary tissue cellular fractions. Food. Chem. Toxicol. 47, 140–144.

Boelsterli, U.A., Ho, H.K., Zhou, S., Leow, K.Y., 2006. Bioactivation and hepatotoxicity of nitroaromatic drugs. Curr. Drug. Metab. 7, 715–727.

Borghoff, S.J., Prescott, J.S., Janszen, D.B., Wong, B.A., Everitt, J.I., 2001. Alpha 2u-globulin nephropathy, renal cell proliferation, and dosimetry of inhaled tert-butyl alcohol in male and female F-344 rats. Toxicol. Sci. 61, 176–186.

Busker, R.W., Beijersbergen van Henegouwen, G.M., 1987. Cytotoxicity and induction of repairable DNA damage by photoactivated 5-nitrofurfural. Toxicology 45, 103–112.

Busker, R.W., Beijersbergen van Henegouwen, G.M., Menke, R.F., Vasbinder, W., 1988. Formation of methemoglobin by photoactivation of nitrofurantoin or of 5-nitrofurfural in rats exposed to UV-A light. Toxicology 51, 255–266.

Cerecetto, H., Di Maio, R., Ibarruri, G., Seoane, G., Denicola, A., Peluffo, G., Quijano, C., Paulino, M., 1998. Synthesis and anti-trypanosomal activity of novel 5-nitro-2-furaldehyde and 5-nitrothiophene-2-carboxaldehyde semicarbazone derivatives. Farmaco 53, 89–94.

Cerecetto, H., González, M., 2011. Antiparasitic prodrug nifurtimox: revisiting its activation mechanism. Future Microbiol. 6, 847–850.

Cheng, K.C., Cahill, D.S., Kasai, H., Nishimura, S., Loeb, L.A., 1992. 8-Hydroxyguanine, an abundant form of oxidative DNA damage, causes G—T and A—C substitutions. J. Biol. Chem. 267, 166–172.

Chung, M.C., Bosquesi, P.L., dos Santos, J.L., 2011. A prodrug approach to improve the physico-chemical properties and decrease the genotoxicity of nitro compounds. Curr. Pharm. 17, 3515–3526.

Cunningham, M.L., 1996. Role of increased DNA replication in the carcinogenic risk of nonmutagenic chemical carcinogens. Mutat. Res. 365, 59–69.

Fleck, L.E., North, E.J., Lee, R.E., Mulcahy, L.R., Casadei, G., Lewis, K., 2014. A screen for a validation of prodrug antimicrobials. Antimicrob. Agents Chemother. 58, 1410–1419.

Hai, A., Kizilbash, N.A., 2013. α(2)-μ-Globulin fragment (a2-f) from kidneys of male rats. Bioinformation 145–149.

Hall, B.S., Bot, C., Wilkinson, S.R., 2011. Nifurtimox activation by trypanosomal type I nitroreductases generates cytotoxic nitrile metabolites. J. Biol. Chem. 286, 13088–13095.

Hiraku, Y., Sekine, A., Nabeshi, H., Midorikawa, K., Murata, M., Kumagai, Y., Kawanishi, S., 2004. Mechanism of carcinogenesis induced by a veterinary antimicrobial drug, nitrofurazone, via oxidative DNA damage and cell proliferation. Cancer Lett. 25, 141–150.

IARC Working Group, 1974. Furaltadone. IARC Monographs on the Evaluation of Carcinogenic Risks to Humans, vol. 7. IARC Working Group, Lyon, France, pp. 161–169.

IARC Working Group, 1983. Furazolidone. IARC Monographs on the Evaluation of the Carcinogenic Risk to Humans, vol. 31. IARC Working Group, Lyon, France, pp. 141–151.

IARC Working Group, 1990a. Nitrofural (nitrofurazone). IARC Monographs on the Evaluation of the Carcinogenic Risks of Chemicals to Humans, vol. 50. IARC Working Group, Lyon, France, pp. 195–209.

IARC Working Group, 1990b. Nitrofurantoin. IARC Monographs on the Evaluation of the Carcinogenic Risks to Humans, vol. 50. IARC Working Group, Lyon, France, pp. 211–231.

Jin, X., Tang, S., Chen, Q., Zou, J., Zhang, T., Liu, F., Zhang, S., Sun, C., Xiao, X., 2011. Furazolidone induced oxidative DNA damage via up-regulating ROS that caused cell cycle arrest in human hepatoma G2 cells. Toxicol. Lett. 201, 205–212.

Kino, K., Sugiyama, H., 2000. GC–>CG transversion mutation might be caused by 8-oxoguanine oxidation product. Nucleic Acids Symp. Ser. 44, 139–140.

Maaland, M., Guardabassi, L., 2011. In vitro antimicrobial activity of nitrofurantoin against *Escherichia coli* and *Staphylococcus pseudintermedius* isolated from dogs and cats. Vet. Microbiol. 151, 396–399.

Matsushita, K., Ishii, Y., Takasu, S., Kuroda, K., Kijima, A., Tsuchiya, T., Kawaguchi, H., Miyoshi, N., Nohmi, T., Ogawa, K., Nishikawa, A., Umemura, T., 2015. A medium-term gpt delta rat model as an in vivo system for analysis of renal carcinogenesis and the underlying mode of action. Exp. Toxicol. Pathol. 67, 31–39.

McCalla, D.R., 1983. Mutagenicity of nitrofuran derivatives: review. Environ. Mutagen. 5, 745–765.

National Toxicology Program (NTP), 1989. NTP Toxicology and Carcinogenesis Studies of nitrofurantoin (CAS No. 67-20-9) in F344/N rats and B6C3F1 mice (Feed Studies). Natl. Toxicol. Program Tech. Rep. Ser. 341, 12–18.

Nohmi, T., Suzuki, T., Masumura, K., 2000. Recent advances in the protocols of transgenic mouse mutation assays. Mutat. Res. 20, 191–215.

Ona, K.R., Courcelle, C.T., Courcelle, J., 2009. Nucleotide excision repair is a predominant mechanism for processing nitrofurazone-induced DNA damage in *Escherichia coli*. J. Bacteriol. 191, 4959–4965.

Quillardet, P., Arrault, X., Michel, V., Touati, E., 2006. Organ-targeted mutagenicity of nitrofurantoin in Big Blue transgenic mice. Mutagenesis 21, 305–311.

Rossi, L., Silva, J.M., McGirr, L.G., O'Brien, P.J., 1988. Nitrofurantoin-mediated oxidative stress cytotoxicity in isolated rat hepatocytes. Biochem. Pharmacol. 37, 3109–3117.

Streeter, A.J., Hoener, B.A., 1988. Evidence for the involvement of a nitrenium ion in the covalent binding of nitrofurazone to DNA. Pharm. Res. 5, 434–436.

Suntres, Z.E., Shek, P.N., 1992. Nitrofurantoin-induced pulmonary toxicity. In vivo evidence for oxidative stress-mediated mechanisms. Biochem. Pharmacol. 43, 1127–1135.

Umemura, T., Kai, S., Hasegawa, R., Kanki, K., Kitamura, Y., Nishikawa, A., Hirose, M., 2003. Prevention of dual promoting effects of pentachlorophenol, an environmental pollutant, on diethylnitrosamine-induced hepato- and cholangiocarcinogenesis in mice by green tea infusion. Carcinogenesis 24, 1105–1109.

Umemura, T., Kanki, K., Kuroiwa, Y., Ishii, Y., Okano, K., Nohmi, T., Nishikawa, A., Hirose, M., 2006. In vivo mutagenicity and initiation following oxidative DNA lesion in the kidneys of rats given potassium bromate. Cancer Sci. 97, 829–835.

Wagenlehner, F.M., Wullt, B., Perletti, G., 2011. Antimicrobials in urogenital infections. Int. J. Antimicrob. Agents 38, 3–10.

Wang, Y., Gray, J.P., Mishin, V., Heck, D.E., Laskin, D.L., Laskin, J.D., 2008. Role of cytochrome P450 reductase in nitrofurantoin-induced redox cycling and cytotoxicity. Free Radic. Biol. Med. 44, 1169–1179.
Wang, Y., Shia, M.A., Christensen, T.G., Borkan, S.C., 2000. Hepatic alpha 2 mu-globulin localizes to the cytosol of rat proximal tubule cells. Kidney Int. 57, 1015–1026.
Williams, G.M., Jeffrey, A.M., 2000. Oxidative DNA damage: endogenous and chemically induced. Regul. Toxicol. Pharmacol. 32, 283–292.
Zorzi, R.R., Jorge, S.D., Palace-Berl, F., Pasqualoto, K.F., Bortolozzo Lde, S., de Castro Siqueira, A.M., Tavares, L.C., 2014. Exploring 5-nitrofuran derivatives against nosocomial pathogens: synthesis, antimicrobial activity and chemometric analysis. Bioorg. Med. Chem. 22, 5844–5852.